Demonstration of a Low-cost Fault Detector for Sum Current Measurement of Overhead MV Lines

Henry Rimminen
Heikki Seppä
Sensors and Wireless Devices – MEMS Sensors
VTT Technical Research Centre of Finland
Espoo, Finland
henry.rimminen@vtt.fi

Antti Kostiainen
Power Systems – Network Management
ABB
Tampere, Finland
antti.kostiainen@fi.abb.com

***Abstract*—We present field test results of a low-cost fault detector for medium voltage power lines. Three devices are clamped on the lines and measure current with induction coils up to 190 A. The sensors harvest energy inductively from the line current. They are synchronized by radio and sum current of three phases is calculated. We compared the measured sum current with a substation reading during earth faults. With fault resistances between 0 - 5000 Ω the full scale error of sum current was between 0.2 - 4.0 %. In a normal state the maximum error was 2.6 %. Earth faults up to 330 Ω were detectable. The energy harvesting provided adequate operating power for the tests, but not yet for continuous operation.**

***Index Terms*--Power distribution faults, Fault detection, Current measurement, Energy harvesting**

I. INTRODUCTION

Affordable wireless sensors hanging from power lines have recently been studied widely [1,2,3]. They typically measure current, voltage and line temperature. Energy harvesting is essential to make them affordable, since conventional fault passage indicators rely on relatively expensive lithium batteries, which also cause indirect maintenance costs. We present actual field test performance of energy harvesting wireless sensors. Three sensors measure current of each phase in a 20 kV power line. They are synchronized by radio, which enables sum current calculation. In unearthed and in compensated networks, detection of faults using sum current is useful, since the earth fault current is often smaller than the load current. Typical fault detectors rely on sensing dynamic phenomena on earth faults [4 - 5]. With sum current measurement, one can set a fixed threshold instead of a dynamic one.

II. IMPLEMENTATION

Fig. 1 (a) shows the implementation of a single detector. The current is measured with a planar coil on the circuit board. It is perpendicular to the magnetic field under measurement but parallel to the fields of neighboring lines. It is separate from the transformer of the harvester to avoid non-linearity due to saturation and to achieve better gain stability. Full scale range is 190 A (RMS) and bandwidth is limited to the fundamental frequency. The waveform is sampled with ATmega644P microcontroller with 10 bit precision and 1200 S/s sample rate (24 samples per 50 Hz cycle). A Bluetooth 2.1 module model WT12 from Bluegiga is used as the radio. The cost of the electronic parts of a single detector is $75 in a small batch excluding the enclosure, which was 3D printed.

Synchronization is crucial for sum current calculation. Rough synchronization of the three devices is done by using the native clock distribution of Bluetooth. This should put the devices on the same 50 Hz cycle. Then each device locks in to the zero-crossing of the 50 Hz current. Samples were sent down to a weather-proof computer and the sum currents were calculated by adding readings from three units.

The energy harvester is a current transformer consisting of an off-the-shelf split ring core, which clamps around the line when the enclosure is closed. A rechargeable battery is needed for two purposes. It provides peak current for the radio and it ensures success of the field test –the harvester was never tested in a real environment before. A 4.8 V 500 mAh Ni-MH battery was used. In a final application, a smaller battery or a super capacitor will be enough.

Fig. 1 (b) shows three detectors installed in Masala, Kirkkonummi, Finland. The lines are non-insulated 20 kV lines (Raven). The network is unearthed and consists of both overhead and underground lines. The field test was arranged by ABB and Fortum, who tested various fault location techniques.

III. RESULTS AND DISCUSSION

A. *Accuracy*

After installation, ±3% relative scale factor variations were present due to tolerances in the line fitting adaptors. These variations were corrected once. The gain is inversely proportional to the distance between the coil and the line and consequently to the fitting tolerance. By introducing a second

This work was funded by CLEEN/SGEM program of TEKES the Finnish funding Agency for Technology and Innovation.

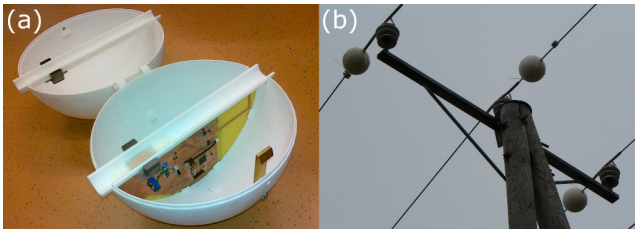

Figure 1. Photographs of (a) one fault detector opened and (b) three detectros installed at the test site at Masala, Kirkkonummi.

coil on the opposite side and connecting the two in series, better initial gain accuracy will be achieved. This is expected to remove the necessity of on-site gain calibration.

On the first fault, a time misalignment was detected. One detector was off by exactly two 50 Hz cycles and one was off by one cycle. This was corrected once. Fig. 2 shows one hour variation of the sum current in a normal state at two times of day. Reference value at the feeder was 0.14 A. In the morning (+3.5 ºC) a safe fault detection threshold is approximately 5 A, which is 2.6 % of full scale. In the afternoon (+10 ºC) a suitable threshold is as low as 2.5 A. We suspect that the normal state variation is caused by temperature dependency of gain and sample time mismatch. Proportions of these error sources are unknown. However, necessity of some kind of temperature compensation is obvious.

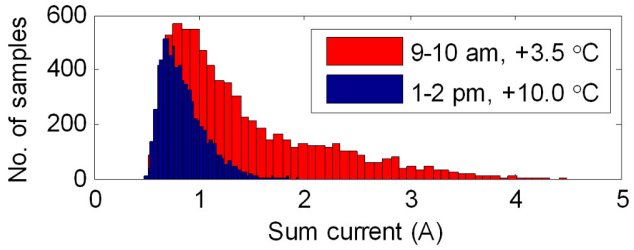

Figure 2. One hour variation of measured sum curent in a normal state.

B. *Earth faults*

The earth faults were on a single phase and lasted for 400 ms. Fault resistance was varied between 0 - 5000 Ω. Fault location was 27 km away from the substation and the detectors were approximately 12 km away from the substation. Load current was 65 A at the feeder and 37 A measured by the detectors. The latter had no reference value.

Fig. 3 shows the measured sum current (DUT) and a reference measurement from the substation (Ref.) with four fault resistances. We calculated error by comparing a 20-cycle RMS value during the fault. The comparison is shown in Table 1. The maximum full scale error is 4 %. The 50 Hz lock-in algorithm causes some of this error. It introduces sample time mismatch when a fault changes the phase of *one* line. This is visible also as post-oscillation in the DUT signals in Fig. 3 (a)-(c). In part (d) the variation before and after the fault is the normal state variation shown in Fig 2.

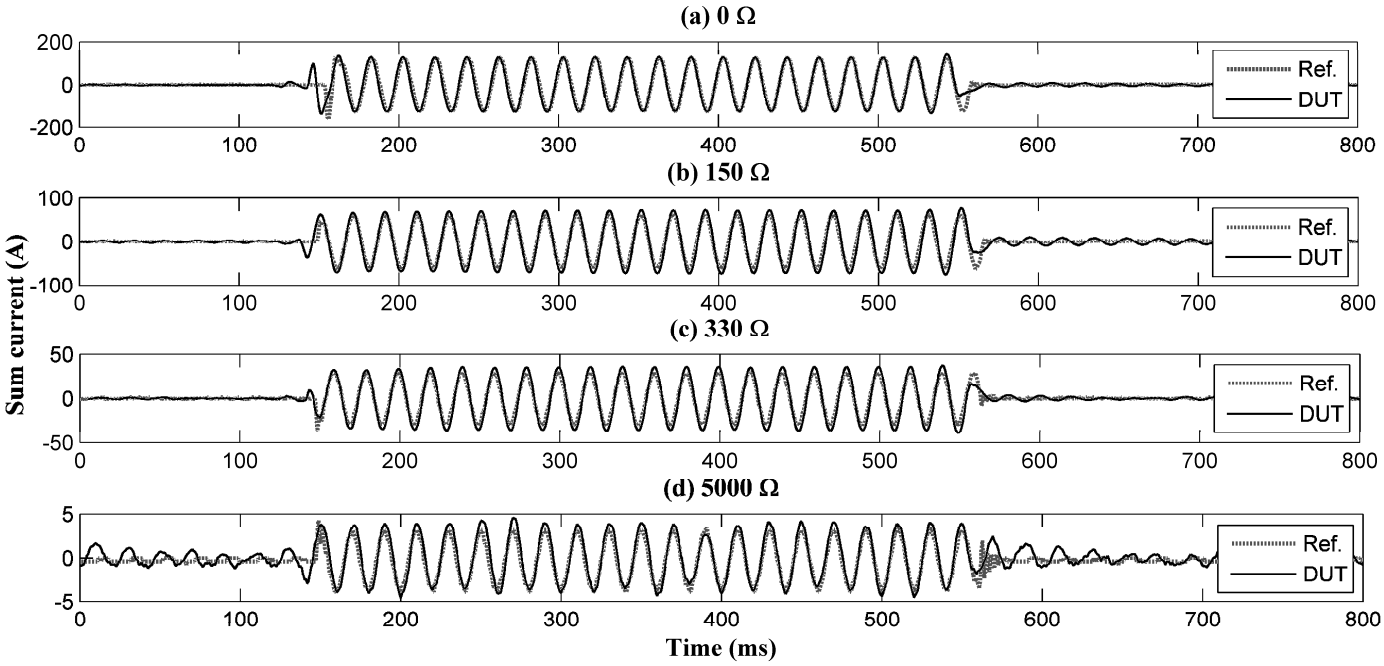

Figure 3. Measurements of single phase earth faults when fault resistance is (a) 0 Ω, (b) 150 Ω, (c) 330 Ω and (d) 5000 Ω.

TABLE I. ERROR ESTIMATION ON EARTH FAULTS

Fault resistance	Sum current on fault		Error	
	Measured	Reference	Abs. error	Rel. error
(Ω)	*(A)*	*(A)*	*(A)*	*(%FS)*
0	91.4	88.2	+ 3.2	1.7
150	51.0	43.4	+ 7.5	4.0
330	25.4	20.7	+ 4.7	2.5
5000	2.8	2.4	+ 0.4	0.2

Now the sample clocks are locked in to the current. In future versions, by locking in to the voltage using an electric field sensor, the fault-induced sample time mismatch is expected to be smaller. Voltage lock-in is also expected to reveal phase change of current during faults.

Faults with resistances between 0 - 330 Ω were clearly detectable. The 5000 Ω fault caused a sum current of 2.8 A, which was not distinct any more. As mentioned before, a safe threshold is approximately 5 A.

C. *Line-to-line fault*

The line-to-line fault lasted for 150 ms. All three lines were connected together with 7 Ω resistors. Fig. 4 shows the waveforms measured by the detectors. They clipped roughly at 275 A (peak). Due to clipping, the measured values were not compared to the reference values.

D. *Energy harvesting*

Laboratory tests preceding the field test indicated adequate power output with resistive loading. Due to some misassumptions concerning the line current level and the loading characteristics of the rechargeable battery, the same power output was not reached in the field test.

Fig. 5 shows the operation hours during three days and average battery voltages at the start and end of each day. During operation the detectors send all samples to the computer at full rate, which is energy intensive. To ensure operation during the test period the detectors were instructed to rest at night time. This is not intended in a final application. When operation time per day is one hour (Mon.), on the next day the battery voltage has risen above the initial value (5.7 V vs. 5.5 V). This duty cycle would enable 'infinite' operation time. When the operation time rises to 4.5 hours (Tue.), the voltage does not rise above the initial voltage (5.6 V vs. 5.7 V). This duty cycle would have eventually depleted the batteries. 3.5 hours seems to be the equilibrium point.

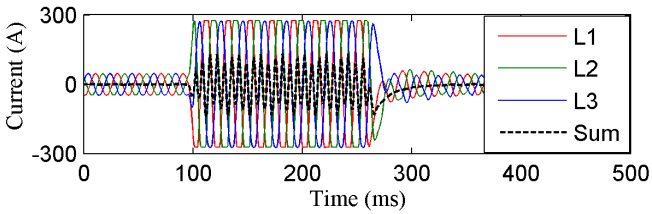

Figure 4. A line-to-line fault measured by the devices under test (DUTs).

To reach continuous sum current measurement, the harvester output must be doubled, the sample rate must be reduced to a couple hundred S/s and the radio must be changed to Bluetooth Low Energy or ZigBee.

E. *Practical problems*

Some practical problems were encountered during the field test. There were intermittent radio transmission failures and parts of the data were lost. A chip antenna was used inside the plastic enclosures. Apparently the moist surface of the enclosure due to rain blocked the radio waves. External rod antennas will be added in future versions. Furthermore, the rain water leaked inside one of the detectors and shorted its battery. Even though the harvester would have eventually recharged the battery, it was replaced for quick continuum of the tests.

IV. CONCLUSIONS

Earth faults with resistances between 0 - 330 Ω were detectable with the proposed device. The normal state variation of the measured sum current was below 5 A, which can be considered as a safe tripping threshold in the final application. One commercial overhead fault passage indicator, which relies on dynamic current sensing on earth faults, has a minimum tripping threshold of 6 A [5].

The second generation device will have several improvements, most likely including a harvester with larger output, an external antenna, a radio with lower power consumption, temperature compensation, dual measurement coils, and voltage locked sampling. These improvements

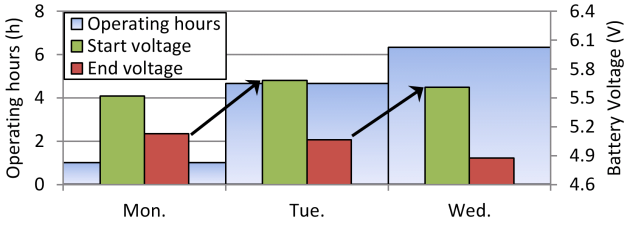

Figure 5. Operating hours per day and battery voltages before and after each day. Arrows indicate effect of harvesting.

would have not been clear without the field test, so it served its purpose well. The second generation device will be also field tested.

ACKNOWLEDGMENT

Special thanks belong to ABB and Fortum, who included VTT in their field test.

REFERENCES

[1] R. Moghe, F.C. Lambert, and D. Divan, "Smart “Stick-on” Sensors for the Smart Grid, " *IEEE Trans. Smart Grid*, vol.3, pp.241-252, Mar. 2012.

[2] F. Kreikebaum, D. Das, Y. Yang, F. Lambert, and D. Divan, "Smart Wires — A distributed, low-cost solution for controlling power flows and monitoring transmission lines," in *proc. 2010 IEEE PES Innovative Smart Grid Technologies Conf. Europe,* 8 p.

[3] Y. Yang, D. Divan, R.G. Harley, and T.G. Habetler, "Design and implementation of power line sensornet for overhead transmission lines," in *proc. 2009 IEEE PES General Meeting,* 8 p.

[4] K.J. Ferreira, and A.E, Emanuel, “A Noninvasive Technique for Fault Detection and Location,” *IEEE Trans. Power Delivery*, vol.25, pp. 3024-3034, Oct. 2010.

[5] Schneider Electric Industries SAS, “Easergy Flite 116-SA,” *Technical data sheet*, 2 p., 2008.